

SMASIS2023-11169

EFFECT OF AREA DENSITY ON SENSITIVITY AND STRAIN SURVIVAL OF REDUCED GRAPHENE OXIDE UNDER LARGE STRAINS

Armin Yazdi
University of Wisconsin
– Milwaukee,
Milwaukee, WI

Li-Chih Tsai
University of Wisconsin
– Milwaukee,
Milwaukee, WI

Nathan Salowitz
University of Wisconsin
– Milwaukee,
Milwaukee, WI

ABSTRACT

Strain sensors are the primary, direct sensing element in many sensors with applications in robotics, wearable sensors, structural health monitoring, and beyond. Cutting edge applications are increasing demand for sensors that can survive and measure large strains (>5%). Presently, the most common strain sensors are composed of a serpentine metal foil which can survive strains up to about 5% with a gauge factor (GF) of about 2 (measured as change in resistance divided by initial resistance all over strain). Research into nanoparticle-based strain sensors commonly reports surviving strains up to 50% and gauge factors around 200. Unfortunately, most nanoparticle-based strain sensors are composed of expensive, toxic materials and require high precision synthesis methods. The reduced Graphene Oxide (rGO) based sensors can be synthesized easily with common materials and methods. Study of strain sensing capabilities have revealed that rGO strain sensors can survive strains beyond 15% with gauge factors (sensitivity) on the order of 200.

Suspensions of graphene oxide (GO)’s flakes were deposited on flexible Polydimethylsiloxane (PDMS) substrates to create specimens with different area densities of 0.69, 0.80 and 0.91 mg/cm² of GO. Specimens were thermally reduced to create rGO-based strain sensors. Resulting sensors were tested under tension applied at a rate of 0.1 mm/sec starting from 0% strain until failure. Resistance of the sensors in the direction aligned with the direction of the applied tension were measured at each

1 mm-increment of tension. Sensitivity and the strain to failure of the sensor were calculated and compared in specimens with different GO area densities.

Our study suggests that with increasing the area density of graphene oxide (GO) during the synthesis of rGO, the survivability of the rGO subjected to large strains can be improved while still demonstrating a high sensitivity. This study can help tailor rGO-based strain sensors especially to the applications where high strain survival (>30%) is required while benefiting from a reasonably good GF (>30)

Keywords: strain sensors, reduced graphene oxide, strain survival, gauge factor.

1. INTRODUCTION

Strain sensors are essential and direct sensing elements that are used in many applications such as aircraft manufacturing, wearable sensors, structural health monitoring, medicine and beyond [1], [2]. Strain gauges with high sensitivity capable of

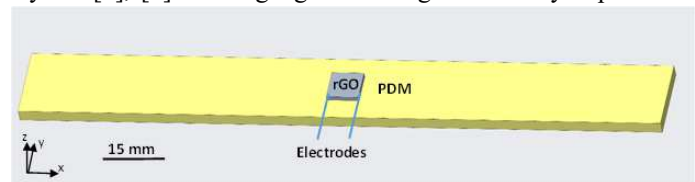


FIGURE 1: rGO as the sensing element on a PDMS substrate

large strain survival are in demand for many futuristic and innovative technologies. Sensitivity in resistive strain gauges is calculated by gauge factor (GF) which is the change of resistance of the strain gauge divided by the initial resistance divided by the value of the strain applied [1], [3]. Strain survival of current commercial foil strain gauges can range from 3% to 5% while showing GF of about 2 [1]. Semiconductor strain gauges have shown a high GF of 100 to 200 and have longer fatigue life compared to foil strain gauges. However, they are very fragile and cannot be used for large strains. Additionally, they are expensive to mass produce and can only be used for special applications [4]–[13]. Nanoparticle strain gauges have shown high gauge factors up to 200 reported while capable of functioning up to 50% strain, reported [11], [14]. Despite the potential benefits of them, scientists have raised concerns about their toxicity [15], [16]. Moreover, their mass production can be economically unfeasible [1], [17]. Reduced graphene oxide (rGO) has shown high strain sensitivity and high strain tolerance while can easily and inexpensively be mass produced [1]. The rGO can be synthesized by several methods using graphene oxide by a process called reduction of graphene oxide [1], [18]–[20]. Oxygen atoms are removed by this process creating low or zero (ideally) oxygen content rGO [21]. Graphene oxide can be reduced using multiple methods including chemical, electrochemical and thermal reduction of the GO [1], [22]–[24]. Chemical reduction of GO can be potentially damaging to the environment and hazardous to human health if due to use of reducing agents like hydrazine [25]. In electrochemical and thermal reduction of GO, electrical voltage and heat energy are used to create rGO respectively. Thermal reduction of GO can be easier than electrochemical reduction of it [1], [20], [26], [27].

Studies on rGO strain sensor under large strains (>5%) are limited. In this study, strain tolerance and sensitivity of rGO strain sensors synthesized by thermal reduction of GO drop-cast on a flexible substrate with 3 different area densities are investigated by application of uniaxial tension and assessment of the resistive response in the direction aligned with the applied tension.

2. MATERIALS AND METHODS

Samples were made with drop-casting of GO on polydimethylsiloxane (PDMS) substrate and thermal reduction of the GO. Specimens were made in three types with different area densities of 0.0069 mg/mm², 0.0080 mg/mm² and 0.0091 mg/mm². Specimens were tested under uniaxial tension up to the point that they lost their electrical conductivity.

To create the samples a method used by M. Rezaee et al. 2021 and L. Tsai et al. 2019 [1], [18]–[20], [28] was implemented. Molds were created using a 3D printer (replicator +). The PDMS substrate was created by casting Dow SYLGARD 186 Silicone Elastomer in the molds allowing it to cure at room temperature for 3 days. Then it was removed from the molds and washed with ultrapure deionized water. The length, thickness and width of the sensor were 127 mm, 2.54 mm, and 15.24 mm respectively. To improve the adhesion of the substrate, it was treated with O2-Plasma for 5 min and then submerged in 2% (3-

Aminopropyl)triethoxysilane and Ethanol for 3 hours. Graphenea 0.4 wt% GO dispersion was shaken in an ultrasonic bath for 2 minutes. 0.0696 ml, 0.0806 ml and 0.0917 ml of the resulting GO were drop-cast into the reservoir area of 6.35 mm by 6.35 mm that was created by the mold to contain the GO in, to create samples with three different area density of 0.0069 mg/mm², 0.0080 mg/mm² and 0.0091 mg/mm² respectively. Samples were allowed to dry for 24 hours at room temperature and placed in an OTF-1200 Series Split Tube Furnaces to thermally be reduced at 180°C for 1 hour and then 200°C for 10 minutes in an argon environment. Then to be able to collect data on the resistance changes of the rGO, two 30-gauge solid copper wires were attached to it using CW2400 conductive epoxy as is shown in Figure 1. Four 15.24 mm by 15.24 mm by 2.54 mm plates were 3D printed using Polylactide (PLA) material. Each end of the samples was sandwiched between two plates to enhance the grip of the substrate for tensile testing.

INSTRON 5980 Series Universal at University of Wisconsin-Milwaukee was used to tension the samples. Each end of the samples was clamped between a couple of jaws of the INSTRON. Tests were performed at the pace of 0.1 mm/sec and resistive response of the sensor was collected at each 1 mm tension increment using a voltage divider with the known resistance of 5.6 kΩ and a TEKTRONIX-MDO3014 Oscilloscope. 5 volt-excitation was provided by an Arduino Uno.

42 samples with three different area densities were tested (14 samples for each). Table 1, 2 and 3 show the distance between electrodes in samples with area densities of 0.0069 mg/mm², 0.0080 mg/mm² and 0.0091 mg/mm² respectively. Average strains of electrical failure and average sensitivity with a linear fit at 7.25% and 19.69% strains were evaluated. In the analysis, output voltage of less than 15 mv was considered an electrical failure.

Table 1. Distance between electrodes in samples with 0.0069 mg/mm² area density

Sample No	Distance between Electrodes (mm)
Sample 1	2.27
Sample 2	1.48
Sample 3	2.26
Sample 4	1.64
Sample 5	1.35
Sample 6	2.95
Sample 7	1.15
Sample 8	2.47
Sample 9	1.8
Sample 10	2.23
Sample 11	2.45
Sample 12	2.3
Sample 13	1.67
Sample 14	2.17

Table 2. Distance between electrodes in samples with 0.0080 mg/mm² area density

Sample No	Distance between Electrodes (mm)
Sample 15	1.79
Sample 16	2.06
Sample 17	1.57
Sample 18	1.97
Sample 19	1.75
Sample 20	2.39
Sample 21	2.02
Sample 22	1.71
Sample 23	2.24
Sample 24	2.28
Sample 25	0.73
Sample 26	1.4
Sample 27	1.64
Sample 28	1.91

Table 3. Distance between electrodes in samples with 0.0091 mg/mm² area density

Sample No	Distance between Electrodes (mm)
Sample 29	1.5
Sample 30	0.84
Sample 31	2.4
Sample 32	0.73
Sample 33	0.72
Sample 34	1.74
Sample 35	2.32
Sample 36	2.11
Sample 37	1.89
Sample 38	1.51
Sample 39	1.84
Sample 40	1.38
Sample 41	1.56
Sample 42	1.88

3. RESULTS AND DISCUSSION

Figures 2, 3 and 4 show the resistive response of the sensor for samples with 0.0069 mg/mm², 0.0080 mg/mm² and 0.0091 mg/mm² respectively.

As can be seen the strain of electrical failure of the sensors increases as the area density increases.

Average strains of electrical failure were 20.36%, 34.19% and 40.92% for samples with 0.0069 mg/mm², 0.0080 mg/mm² and 0.0091 mg/mm² respectively which showed an increase in strains of electrical failure as the area density of samples increased. At 7.25% strain, samples with area densities of 0.0069, 0.0080, 0.0091 mg/mm² showed average GFs of 40.14(Ω/Ω)/(m/m), 35.63(Ω/Ω)/(m/m), and 28.66(Ω/Ω)/(m/m), respectively and at 19.69% strain, they showed average GFs of 78.39(Ω/Ω)/(m/m), 65.54(Ω/Ω)/(m/m), and 36.49(Ω/Ω)/(m/m). It showed that the sensitivity of the sensor with increase in area density decreased. However, the sensor still possessed a high sensitivity to strain in comparison to common foil strain gauges with the GF of about 2.

4. CONCLUSION

This study showed that the samples with increased area densities showed a greater average strain of electrical failure. The gauge factor (sensitivity) of the sensor reduced by increase in their area density. However, the sensor still possessed a high sensitivity to strain compared to common foil strain gauges with the GF of about 2. This study showed that the area density of the rGO could be manipulated for its properties like strain tolerance and sensitivity to be tailored to the desired values for different applications.

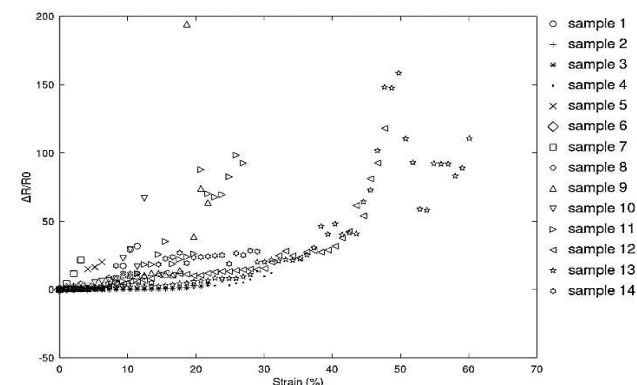


FIGURE 2: Resistive response of the sensors with 0.0069 mg/mm² area density

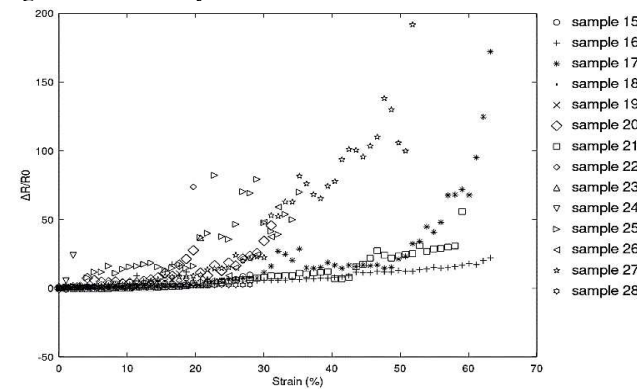


FIGURE 3: Resistive response of the sensors with 0.0080 mg/mm² area density

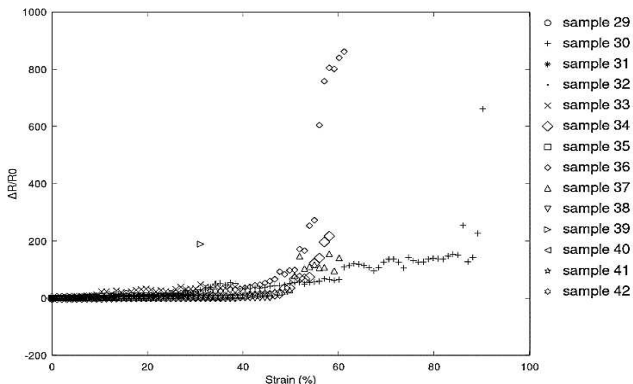


FIGURE 4: Resistive response of the sensors with 0.0091 mg/mm² area density

5. FUTURE WORK

Deformation of the rGO sensor will be investigated under the confocal microscope for samples with different area densities.

ACKNOWLEDGEMENTS

This project was supported by The Water Equipment & Policy Research Center (WEP) located at University of Wisconsin-Milwaukee and Marquette University. WEP operates under the auspices of the National Science Foundation Industry/University Cooperative Research Center Program. This project was also mentored by following companies: Badger Meter and Zurn/Rexnord, Sloan, A.O Smith, Watts Water, GE Appliance and Pentair.

REFERENCES

- [1] A. Yazdi, L.-C. Tsai, and N. Salowitz, “Investigation of the Resistive Response of Reduced Graphene Oxide for Sensing Large Strains (>10%),” in *ASME 2022 Conference on Smart Materials, Adaptive Structures and Intelligent Systems*, American Society of Mechanical Engineers, Sep. 2022. doi: 10.1115/SMASIS2022-90349.
- [2] A. Serban and P. D. Barsanescu, “Automatic Detection of the Orientation of Strain Gauges Bonded on Composite Materials with Polymer Matrix, in Order to Reduce the Measurement Errors,” *Polymers (Basel)*, vol. 15, no. 4, p. 876, Feb. 2023, doi: 10.3390/polym15040876.
- [3] J. Fraden, *Handbook of Modern Sensors*, 4th ed. New York, NY: Springer New York, 2010. doi: 10.1007/978-1-4419-6466-3.
- [4] S. M. Won *et al.*, “Piezoresistive Strain Sensors and Multiplexed Arrays Using Assemblies of Single-Crystalline Silicon Nanoribbons on Plastic Substrates,” *IEEE Trans Electron Devices*, vol. 58, no. 11, pp. 4074–4078, Nov. 2011, doi: 10.1109/TED.2011.2164923.
- [5] M. Ying *et al.*, “Silicon nanomembranes for fingertip electronics,” *Nanotechnology*, vol. 23, no. 34, p. 344004, Aug. 2012, doi: 10.1088/0957-4484/23/34/344004.
- [6] D.-H. Kim *et al.*, “Electronic sensor and actuator webs for large-area complex geometry cardiac mapping and therapy,” *Proceedings of the National Academy of Sciences*, vol. 109, no. 49, pp. 19910–19915, Dec. 2012, doi: 10.1073/pnas.1205923109.
- [7] S. Yang and N. Lu, “Gauge Factor and Stretchability of Silicon-on-Polymer Strain Gauges,” *Sensors*, vol. 13, no. 7, pp. 8577–8594, Jul. 2013, doi: 10.3390/s130708577.
- [8] M. Bao, “Introduction to MEMS Devices,” in *Analysis and Design Principles of MEMS Devices*, Elsevier, 2005, pp. 1–32. doi: 10.1016/b978-044451616-9/50002-3.
- [9] M.-H. Bao, *Micro Mechanical Transducers - Pressure Sensors, Accelerometers and Gyroscopes*, 1st ed. Amsterdam ; New York: Elsevier, 2000.
- [10] M. Bao, “Mechanics of Beam and Diaphragm Structures,” *Analysis and Design Principles of MEMS Devices*, pp. 33–114, Jan. 2005, doi: 10.1016/B978-044451616-9/50003-5.
- [11] J. L. Tanner, D. Mousadakos, P. Broutas, S. Chatzandroulis, Y. S. Raptis, and D. Tsoukalas, “Nanoparticle Strain Sensor,” *Procedia Eng*, vol. 25, pp. 635–638, 2011, doi: <https://doi.org/10.1016/j.proeng.2011.12.158>.
- [12] K. K. Ng, “Strain Gauge,” in *Complete Guide to Semiconductor Devices*, Hoboken, NJ, USA: John Wiley & Sons, Inc., 2010, pp. 544–550. doi: 10.1002/9781118014769.ch72.
- [13] J. X. J. Zhang and K. Hoshino, *Molecular Sensors and Nanodevices, Principles, Designs and Applications in Biomedical Engineering*. Elsevier, 2019. doi: 10.1016/C2017-0-02290-5.
- [14] N. M. Sangeetha, N. Decorde, B. Viallet, G. Viau, and L. Ressier, “Nanoparticle-Based Strain Gauges Fabricated by Convective Self Assembly: Strain Sensitivity and Hysteresis with Respect to Nanoparticle Sizes,” *The Journal of Physical Chemistry C*, vol. 117, no. 4, pp. 1935–1940, Jan. 2013, doi: 10.1021/jp310077r.
- [15] J. T. Buchman, N. V. Hudson-Smith, K. M. Landy, and C. L. Haynes, “Understanding Nanoparticle Toxicity Mechanisms To Inform Redesign Strategies To Reduce Environmental Impact,” *Acc Chem Res*, vol. 52, no. 6, pp. 1632–1642, Jun. 2019, doi: 10.1021/acs.accounts.9b00053.
- [16] L. Ou *et al.*, “Toxicity of graphene-family nanoparticles: a general review of the origins and mechanisms,” *Part Fibre Toxicol*, vol. 13, no. 1, p. 57, 2016, doi: 10.1186/s12989-016-0168-y.
- [17] H. M. Soe, A. A. Manaf, A. Matsuda, and M. Jaafar, “Development and fabrication of highly flexible, stretchable, and sensitive strain sensor for long durability based on silver nanoparticles–polydimethylsiloxane

composite,” *Journal of Materials Science: Materials in Electronics*, vol. 31, no. 14, pp. 11897–11910, Jul. 2020, doi: 10.1007/s10854-020-03744-6.

[18] L.-C. Tsai, M. Rezaee, M. I. Haider, A. Yazdi, and N. P. Salowitz, “Quantitative measurement of thin film adhesion force,” in *ASME 2019 Conference on Smart Materials, Adaptive Structures and Intelligent Systems, SMASIS 2019*, 2019, doi: 10.1115/SMASIS2019-5615.

[19] M. Rezaee, L.-C. Tsai, M. I. Haider, A. Yazdi, E. Sanatizadeh, and N. P. Salowitz, “Quantitative peel test for thin films/layers based on a coupled parametric and statistical study,” *Sci Rep*, vol. 9, no. 1, 2019, doi: 10.1038/s41598-019-55355-9.

[20] M. Rezaee, L. Chih Tsai, A. Elyasigorji, M. Istiaque Haider, A. Yazdi, and N. P. Salowitz, “Quantification of the Mechanical Strength of Thermally Reduced Graphene Oxide Layers on Flexible Substrates,” *Eng Fract Mech*, p. 107525, Jan. 2021, doi: 10.1016/j.engfracmech.2021.107525.

[21] W. Liu and G. Speranza, “Tuning the Oxygen Content of Reduced Graphene Oxide and Effects on Its Properties,” *ACS Omega*, vol. 6, no. 9, pp. 6195–6205, Mar. 2021, doi: 10.1021/acsomega.0c05578.

[22] D. Karačić *et al.*, “Electrochemical reduction of thin graphene-oxide films in aqueous solutions – Restoration of conductivity,” *Electrochim Acta*, vol. 410, p. 140046, Apr. 2022, doi: 10.1016/j.electacta.2022.140046.

[23] E. P. Randviir, D. A. C. Brownson, and C. E. Banks, “A decade of graphene research: production, applications and outlook,” *Materials Today*, vol. 17, no. 9, pp. 426–432, Nov. 2014, doi: 10.1016/j.mattod.2014.06.001.

[24] S. Azizighannad and S. Mitra, “Stepwise Reduction of Graphene Oxide (GO) and Its Effects on Chemical and Colloidal Properties,” *Sci Rep*, vol. 8, no. 1, p. 10083, Dec. 2018, doi: 10.1038/s41598-018-28353-6.

[25] S. Y. Toh, K. S. Loh, S. K. Kamarudin, and W. R. W. Daud, “Graphene production via electrochemical reduction of graphene oxide: Synthesis and characterisation,” *Chemical Engineering Journal*, vol. 251, pp. 422–434, Sep. 2014, doi: 10.1016/j.cej.2014.04.004.

[26] W. J. Basirun, M. Sookhakian, S. Baradaran, M. R. Mahmoudian, and M. Ebadi, “Solid-phase electrochemical reduction of graphene oxide films in alkaline solution,” *Nanoscale Res Lett*, vol. 8, no. 1, p. 397, 2013, doi: 10.1186/1556-276X-8-397.

[27] S. Chong, C. Lai, and S. Abd Hamid, “Controllable Electrochemical Synthesis of Reduced Graphene Oxide Thin-Film Constructed as Efficient Photoanode in Dye-Sensitized Solar Cells,” *Materials*, vol. 9, no. 2, p. 69, Jan. 2016, doi: 10.3390/ma9020069.

[28] Maysam Rezaee, “Bonding Evaluation of Graphene-Oxide Layers on Flexible Substrates,” University of Wisconsin Milwaukee, 2021.